Thermal Stress Analysis of Multi-layer Thin Films and Coatings by an Advanced Boundary Element Method

Xiaolin Chen and Yijun Liu[1]

Abstract: An advanced boundary element method (BEM) is developed in this paper for analyzing thin layered structures, such as thin films and coatings, under the thermal loading. The boundary integral equation (BIE) formulation for steady-state thermoelasticity is reviewed and a special case, that is, the BIE for a uniform distribution of the temperature change, is presented. The new nearly-singular integrals arising from the applications of the BIE/BEM to thin layered structures under thermal loading are treated in the same way as developed earlier for thin structures under the mechanical loading. Three 2-D test problems involving layered thin films and coatings on an elastic body are studied using the developed thermal BEM and a commercial FEM software. Numerical results for displacements and interfacial stresses demonstrate that the developed BIE/BEM remains to be very accurate, efficient in modeling, and surprisingly stable, for thin elastic materials with the thickness-to-length ratios down to 10^{-9} (the nano-scale). This thermal BEM capability can be employed to investigate other more important and realistic thin film and coating problems, such as residual stresses, interfacial crack initiation and propagation (peeling-off), in electronic packaging or other engineering applications.

1 Introduction

The boundary element method (BEM), based on the boundary integral equation (BIE) formulation, is well known for its accuracy and efficiency in stress analysis (see, for example, the early work in Refs. (Rizzo 1967; Rizzo and Shippy 1977)) and many other engineering applications (Mukherjee 1982; Cruse 1988; Brebbia and Dominguez 1989; Banerjee 1994; Kane 1994). In recent years, the BEM has also been found to be espe-

cially accurate and efficient in the analysis of thin elastic structures or materials, once the nearly-singular integrals existing in the BIE for such applications are computed accurately (Cruse and Aithal 1993; Huang and Cruse 1993; Katsikadelis and Nerantzaki 2000; Liu, Zhang et al. 1993; Liu 1998; Luo, Liu et al. 1998; Nikishkov, Park, and Atluri 2001; Mukherjee, Chati et al. 2000). Applications of the BEM to thin shell-like structures, thin films and coatings, interphases in composites, and sound and shell structure interactions have been successfully studied using the corresponding BIE formulations and the BEM, under the mechanical loading (Liu 1998; Luo, Liu et al. 1998; Chen and Liu 1999; Chen, Liu et al. 2000; Liu and Xu 2000; Liu, Xu et al. 2000; Luo, Liu et al. 2000; Chen and Liu 2001). It is a natural and important extension to develop the BEM capabilities for thin elastic structures or materials under the thermal loading which has significant implications in, for example, electronic packaging and aerospace engineering applications.

Computational methods have been applied to analyze the thin films and coatings for quite some time. Some of the recent applications of the finite element method (FEM) for thin films or coatings under the thermal loading can be found in Refs. (Igic and Mawby 1998; Abedian, Szyszkowski et al. 1999; Cheng, Yang et al. 1999; Igic and Mawby 1999; Liu, Suo et al. 1999). All of these FEM studies show that very fine finite element mesh is essential in order to accurately evaluate the interfacial stresses in thin films and coatings. For cases involving singular fields, such as interfacial cracks or stresses near the free edge of an interface, even more elements are required, which can quickly make the domain-based FEM approach costly or inefficient.

On the other hand, there are very few studies, reported only recently, using the BEM for the analysis of thin films and coatings, especially under the thermal loading. In Ref. (Gray, Maroudas et al. 1998), a Galerkin BIE/BEM is developed to accurately evaluate the deriva-

[1] Department of Mechanical Engineering
University of Cincinnati, P.O. Box 210072
Cincinnati, Ohio 45221-0072, U.S.A.
E-mail: yijun.liu@uc.edu

tives of the fields (such as stresses), and in Ref. (Gray, Maroudas et al. 1999), the BEM based on an approximate Green's function is developed. Both of these BEM approaches are applied successfully to the problem of electromigration-driven void dynamics in metallic thin-film interconnects (Gray, Maroudas et al. 1998; Gray, Maroudas et al. 1999). In Ref. (Hu, Li et al. 1998), a coating on an elastic substrate under a uniform change in temperature is studied using the commercial BEM software BEASY, with the smallest thickness-to-length ratio for the coating being 0.025. Detailed studies of the singular stress fields near the free edges of the bi-material interface are performed and the failure criterion for a coated structure is also discussed in Ref. (Hu, Li et al. 1998). In all the above BEM studies of thin films or coatings, the difficulty of dealing with nearly-singular integrals in such applications of the BEM are not addressed. It is believed that, once the nearly-singular integrals are resolved in the BEM, much larger, and hence fewer, boundary elements can be employed in the BEM mesh in regions away from the singular fields. This will improve the efficiency of the BEM for analyzing thin films and coatings with arbitrarily small thickness-to-length ratios, as demonstrated in Refs. (Luo, Liu et al. 1998; Luo, Liu et al. 2000) in the context of elastostatic BIE. Dealing with the nearly-singular integrals accurately and efficiently in the thermoelasticity BIE will be the focus of the current study reported herein.

In this paper, the advanced BEM developed in (Luo, Liu et al. 1998; Luo, Liu et al. 2000) is extended to the thermoelasticity BIE, in order to analyze thin layered structures, such as thin films and coatings, under the thermal loading. The BIE formulation for steady-state thermoelasticity is reviewed first, and then a special case, that is, the BIE for a uniform distribution of the temperature change, is presented. The new nearly-singular integrals arising from the applications of the BIE/BEM to thin layered structures under the thermal loading are treated in the same way as developed earlier for thin structures under the mechanical loading. Three 2-D test problems involving thin films and coatings on an elastic body are studied using the developed thermal BEM and a commercial FEM software. The numerical results demonstrate that the developed BIE/BEM for thermal stress analysis of thin layered structures is very accurate, efficient in modeling, and surprisingly stable, for thin elastic materials with the thickness-to-length ratios in the $10^{-9} - 10^{-12}$

range. Applications of the developed thermal BEM with thin-body capabilities are quite promising, for example, in analyzing residual stresses, interfacial crack initiation and propagation (peeling-off) in various thin films and coatings employed in electronic packaging and other engineering practices.

2   The BIE formulations for thermoelasticity problems

We first review the boundary integral equation formulation for the general steady-state thermoelasticity problems. Then we focus on a special BIE formulation for the analysis of thin layered structures where the temperature change is constant across the spatial domain.

The general governing equations in thermoelasticity for linearly elastic and isotropic materials are as follows:

$$\sigma_{ij,j} = 0, \tag{1}$$

$$\sigma_{ij} = E_{ijkl}(\varepsilon_{kl} - \alpha \Delta T \delta_{kl}), \tag{2}$$

$$\varepsilon_{ij} = \frac{1}{2}(u_{i,j} + u_{j,i}), \tag{3}$$

where (mechanical) body forces have been ignored; σ_{ij}, ε_{ij}, and u_i are the stress, (total) strain, and displacement fields, respectively; E_{ijkl} the Young's modulus tensor; α the coefficient of thermal expansion; Δ the change of temperature in the elastic material occupying the domain V (Fig. 1); and δ_{ij} the Kronecker δ symbol. The above equations are valid for 3-D thermal stress analysis and will be solved under given boundary conditions. For 2-D plane strain problems, the coefficient of thermal expansion α in Eq. (2) should be replaced by $(1 + \nu)\alpha$, with ν being the Poisson's ratio of the material.

To establish the BIE corresponding to the differential equations (1-3), we consider the fundamental solution at the field point P in an infinite elastic medium due to a concentrate unit force applied at a source point P_0 (*no thermal effects* are included). The stress field $\Sigma_{ijk}(P, P_0)$ of this fundamental solution satisfies the following equilibrium equation:
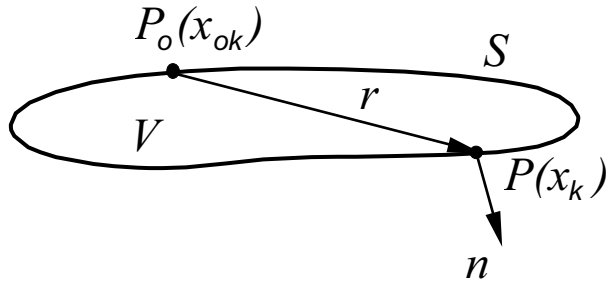
Figure 1 : A domain *V* with boundary *S*.

$$\Sigma_{ijk,k}(P,P_0) + \delta_{ij}\delta(P,P_0) = 0, \tag{4}$$

where the Dirac δ function $\delta(P, P_0)$ represents the unit concentrate force and the index i indicates the direction of that unit force.

Applying the Gauss theorem, we obtain the following identity (or a reciprocal relation) involving both the solution satisfying Eqs. (1-3) (with thermal effects) and the fundamental solution (without thermal effects):

$$\int_V (\sigma_{jk,k}U_{ij} - \Sigma_{ijk,k}u_j)dV =$$

$$\int_S (U_{ij}t_j - T_{ij}u_j)dS + \int_V \Sigma_{ijj}\alpha\Delta T dV, \tag{5}$$

where U_{ij} is the displacement field in the fundamental solution; t_j and T_{ij} are the tractions in the solution of Eqs. (1-3) and the fundamental solution, respectively. Substituting Eqs. (1) and (4) into the left-hand side of Eq. (5), we obtain the following *representation integral* for the displacement field:

$$u_i(P_0) = \int_S [U_{ij}(P,P_0)t_j(P) - T_{ij}(P,P_0)u_j(P)] dS(P)$$

$$+ \int_V \Sigma_{ijj}(P,P_0)\alpha\Delta T dV(P), \quad \forall P_0 \in V. \tag{6}$$

Notice that if there is no temperature change in the material, that is, $\Delta T = 0$, then the last volume integral in (6)

vanishes and the representation integral is identical to the one for elasticity problems without the thermal loading.

Letting the source point P_0 go to the boundary S in Eq. (6), we obtain the following "boundary" integral equation for thermoelasticity problems:

$$C_{ij}(P_0)u_j(P_0) = \int_S [U_{ij}(P,P_0)t_j(P) - T_{ij}(P,P_0)u_j(P)] dS(P)$$

$$+ \int_V \Sigma_{ijj}(P,P_0)\alpha\Delta T dV(P), \quad \forall P_0 \in S, \tag{7}$$

where the values of the coefficient C_{ij} depend on the smoothness of boundary S at point P_0 (e.g., $C_{ij}(P_0) = \frac{1}{2}\delta_{ij}$, if S is smooth). However, these values of C_{ij} and the singular integrals containing the T_{ij} kernel do not need to be computed directly in the BIEs, as discussed in Refs. (Cruse 1974; Liu and Rudolphi 1991; Liu 2000).

The treatment of the volume integral in Eq. (7) has been the focus in the thermoelasticity BIE and will be discussed in detail. Applying the stress-strain and strain-displacement relations (without the thermal effects) for the fundamental solution, and the Gauss theorem, we have the following results for evaluating the volume integral in Eq. (7):

$$\int_V \Sigma_{ijj}\alpha\Delta T dV = \int_V E_{jjkl}U_{ik,l}\alpha\Delta T dV$$

$$= \int_V [E_{jjkl}U_{ik}\alpha\Delta T]_{,l}dV - \int_V E_{jjkl}U_{ik}(\alpha\Delta T)_{,l}dV$$

$$= \int_S E_{jjkl}U_{ik}n_l\alpha\Delta T dS - \int_V E_{jjkl}U_{ik}(\alpha\Delta T)_{,l}dV.$$

For isotropic materials, the Young's modulus tensor is in the form:

$$E_{ijkl} = \frac{2G\nu}{1-2\nu}\delta_{ij}\delta_{kl} + G(\delta_{ik}\delta_{jl} + \delta_{il}\delta_{jk}),$$

for both 3-D and 2-D plane strain problems, where G is the shear modulus.

For 3-D problems, we have

$$E_{jjkl} = \frac{2G\nu}{1-2\nu}3\delta_{kl} + G(\delta_{kl} + \delta_{kl}) = \frac{2(1+\nu)G}{1-2\nu}\delta_{kl},$$

Substituting this into the above result for the volume integral, we obtain:

$$\int_V \Sigma_{ijj} \alpha \Delta T \, dV = \gamma \int_S U_{ij} n_j \Delta T \, dS - \gamma \int_V U_{ij} (\Delta T)_{,j} dV, \quad (8)$$

where the constant γ is given by:

$$\gamma = \frac{2(1+\nu) G \alpha}{1 - 2\nu}. \quad (9)$$

Thus, BIE (7) becomes:

$$C_{ij}(P_0) u_j(P_0) = \int_S [U_{ij}(P,P_0) t_j(P) - T_{ij}(P,P_0) u_j(P)] dS(P)$$

$$+ \gamma \int_S U_{ij}(P,P_0) n_j(P) \Delta T(P) dS$$

$$- \gamma \int_V U_{ij}(P,P_0) [\Delta T(P)]_{,j} dV, \quad \forall P_0 \in S, \quad (10)$$

for 3-D problems. It can be verified that this BIE, with γ given in (9), is also valid for *plane strain* problems for which the indices have the range of 1 to 2. From this equation, it can be concluded that the effect of temperature change ΔT in an elastic body is equivalent to adding a body force equal to $(-\gamma[\Delta T]_{,j})$ and a traction equal to $(\gamma \Delta T n_j)$ (see, e.g., Ref. (Brebbia and Dominguez 1989), p. 171). BIE (10) still contains one volume integral which has to be converted into a boundary one.

Introducing the Galerkin vector G_{ij} such that the fundamental solution U_{ij} can be written in the following form:

$$U_{ij} = G_{ij,kk} - \frac{1}{2(1-\nu)} G_{ik,jk},$$

we can convert the domain integral in BIE (10) into a boundary integral to obtain the following BIE for steady-state thermoelasticity problems (see, e.g., (Brebbia and Dominguez 1989)):

$$C_{ij}(P_0) u_j(P_0) = \int_S [U_{ij}(P,P_0) t_j(P) - T_{ij}(P,P_0) u_j(P)] dS(P)$$

$$+ \frac{(1-2\nu)\gamma}{2(1-\nu)} \left\{ \int_S G_{ij,jk}(P,P_0) n_k(P) \Delta T(P) dS \right.$$

$$\left. - \int_S G_{ij,j}(P,P_0) [\Delta T(P)]_{,k} n_k(P) dS \right\}, \quad \forall P_0 \in S, \quad (11)$$

in which all integrals are now on the boundary S. This is a *general* BIE for steady-state thermoelasticity analysis in which the spatial variations of the temperature changes can be accounted for.

If the temperature change is uniform across the elastic body (no spatial variations), then $\Delta T =$ constant, and the last integral in BIE (11) vanishes. However, in this special case, a better choice of the BIEs is to use Eq. (10) without the last integral, that is,

$$C_{ij}(P_0) u_j(P_0) = \int_S [U_{ij}(P,P_0) t_j(P) - T_{ij}(P,P_0) u_j(P)] dS(P)$$

$$+ \gamma \Delta T \int_S U_{ij}(P,P_0) n_j(P) dS, \quad \forall P_0 \in S, \quad (12)$$

in which the integral due to the uniform temperature change is almost identical to the first integral and hence can be dealt with in a similar way in the numerical procedure.

The thermoelastic BIE, in the form of Eq. (12) for uniform temperature changes, will be applied for the analysis of thin layered structures, such as thin films and coatings, under the thermal loading. Although in real engineering applications the temperature changes can be vastly different at different locations of a structure, there are indeed many cases where the temperature changes can be assumed safely as uniform across the structure or material domain, especially if the temperature field is steady state and the dimension of the structure is small.

Before BIE (12) can be applied to analyze thin films and coatings under thermal loading, we must address the problem of how to accurately compute the nearly-singular integrals in BIE (12) for such applications. As in the BEM analysis of thin layered structures or materials

under mechanical loading, the most difficult part in such analysis is the treatment of the nearly-singular integrals existing in the BIE when integrations need to be done on one surface while the source point is on the other closely nearby surface. Efficient analytical and numerical procedures have been devised for computing such nearly-singular integrals for both 3-D (Liu, Zhang et al. 1993; Liu 1998) and 2-D (Luo, Liu et al. 1998) stress analysis problems under the mechanical loading (see, also, Ref. (Mukherjee, Chati et al. 2000) for a recent review and some new results in dealing with the various nearly-singular integrals). In this paper, these techniques in dealing with nearly-singular integrals in the BIEs are extended to the thermoelasticity BIE. Specifically, for the 2-D thermoelastic BIE (Eq. (12)), the techniques developed in Ref. (Luo, Liu et al. 1998) are extended to deal with the last integral in Eq. (12) which is simply a variation of the first integral in this form of the BIE. Details of the techniques in dealing with the nearly-singular integrals in the BIE for 2-D elasticity problems can be found in Ref. (Luo, Liu et al. 1998).

To understand how the last integral in BIE (12) can be treated in a similar way as for the first integral, the discretization of the BIE (12) is discussed briefly. By the standard discretization procedure in the BEM, the discretized form of BIE (12), using, for example, quadratic boundary elements, can be written in the following form:

$$
\mathbf{C}_i \mathbf{u}_i = [\mathbf{G}_{i1} \quad \mathbf{G}_{i2} \quad \cdots \quad \mathbf{G}_{iN}] \begin{Bmatrix} \mathbf{t}_1 \\ \mathbf{t}_2 \\ \vdots \\ \mathbf{t}_N \end{Bmatrix}
$$

$$
- [\hat{\mathbf{H}}_{i1} \quad \hat{\mathbf{H}}_{i2} \quad \cdots \quad \hat{\mathbf{H}}_{iN}] \begin{Bmatrix} \mathbf{u}_1 \\ \mathbf{u}_2 \\ \vdots \\ \mathbf{u}_N \end{Bmatrix} + \mathbf{b}_i^{\text{Therm}}, \quad (13)
$$

when source point P_0 is placed at node i, where the vector due to the thermal effect (the third integral in BIE (12)) is:

$$
\mathbf{b}_i^{Therm} = \gamma \Delta T [\mathbf{G}_{i1} \quad \mathbf{G}_{i2} \quad \cdots \quad \mathbf{G}_{iN}] \begin{Bmatrix} \mathbf{n}_1 \\ \mathbf{n}_2 \\ \vdots \\ \mathbf{n}_N \end{Bmatrix}, \quad (14)
$$

N is the total number of the nodes on the boundary; $\mathbf{u}$, $\mathbf{t}$ and $\mathbf{n}$ are the displacement, traction and normal vectors at each node, respectively; and $\mathbf{C}$, $\mathbf{G}$ and $\mathbf{H}$ are sub-matrices corresponding to the coefficient C_{ij}, U_{ij} and T_{ij} kernels, respectively (see, e.g., Ref. (Brebbia and Dominguez 1989)). Combining all the equations at the N nodes on the boundary and applying the mechanical boundary conditions, the final BEM system of equations can be written as:

$$
\mathbf{A}\mathbf{x} = \mathbf{b} + \mathbf{b}^{Therm}, \quad (15)
$$

where $\mathbf{A}$ is the coefficient matrix, $\mathbf{x}$ the unknown vector, and $\mathbf{b}$ the load vector due to the mechanical boundary conditions. From this equation, we can observe that the thermal effects act like an additional load to the structure.

To analyze multi-domain problems, BIE (12), or in the discretized form, Eq. (15), is applied to each material domain, such as different layers of thin films or coatings. Each BIE relates the boundary displacement and traction fields in that domain only. The resulting BIEs from each domain are then combined through the interface conditions, for example, continuity of the displacement and traction at a perfectly bonded interface (Liu, Xu et al. 2000). A combined linear system of equations, containing all the equations from all the material domains, is solved to obtain the displacement and traction fields at the boundary and all material interfaces (Liu, Xu et al. 2000; Luo, Liu et al. 2000).

3 Numerical verification

Several test problems are presented in this section, first to verify the developed thermal BEM code for 2-D problems, then to demonstrate the efficiency and accuracy of the BEM code as compared with the FEM. Quadratic boundary elements are employed in all the examples.

3.1 A thin film under thermal loading

We first test the BEM on the thermal stress analysis of a thin film model, as shown in Fig. 2, for which the exact solution is readily available. The *plane strain condition* is assumed and all the boundary of the film is constrained in the normal direction (roller support). The material constants used are:

Young's modulus $E = 4.0$ GPa;
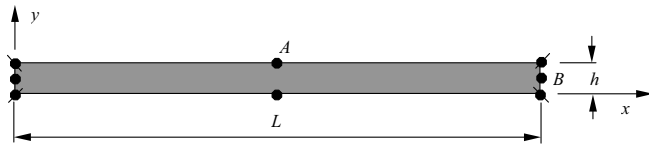
Figure 2 : A thin film constrained at all edges and discretized with *four* boundary elements.

Poisson's ratio $v = 0.34$;

Coefficient of thermal expansion $\alpha = 10.0 \times 10^{-6}/°C$.

A uniform temperature change $\Delta T = 100 °C$ is applied to the film. Under these conditions, the exact solution of the thermal stresses in the film is found to be:

$\sigma_x = \sigma_y = -\frac{E\alpha\Delta T}{1-2v} = -12.5$ MPa; and $\tau_{xy} = 0$.

For the BEM analysis, the boundary of the film is discretized using only *four* quadratic elements, one on each side. The BEM results are presented in Table 1 for different values of the thickness h. As we can observe from these results, the developed thermal BEM code is extremely accurate and efficient for this case. Stable BEM results are obtained for values of the thickness h ranging from L (a square) to $10^{-16} L$ (an extremely thin film) using the same *four* element BEM model. Marked errors of the BEM results are observed only when h reaches the small values of $10^{-15} L$ and $10^{-16} L$. Although the stress distribution in this case is very simple (constant), the demand on the BEM to compute this distribution accurately is not trivial at all, since all the integrals must be evaluated very accurately in order to achieve the high accuracy. This high accuracy and efficiency of the advanced BEM for thin shell-like structures or materials with the thickness below the nano-scales were first demonstrated in Refs. (Luo, Liu et al. 1998; Luo, Liu et al. 2000) for thin films and coatings, and in Refs. (Liu and Xu 2000; Liu, Xu et al. 2000; Chen and Liu 2001) for composite materials, under mechanical loading.

It should be pointed out that in this example, the extremely small values used for the thickness h, although relative to the dimension L, could easily violate the assumptions in elasticity which regards the material as a continuum. The elasticity theory cannot deal with materials with sizes approaching that of an atom or molecule. However, the main concern here is to verify the BIE formulation and the BEM procedure developed for analyzing thin structures or materials under thermal loading. The applicability of the developed BEM capabilities (in
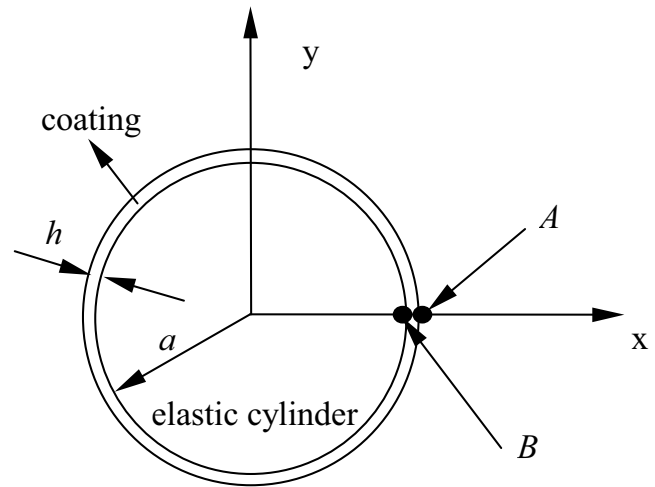
Figure 3 : An elastic cylinder with a thin coating.

fact, that of the elasticity theory) should be judged when it is applied to a given problem.

3.2 Thin coatings on an elastic cylinder

Next, we study an elastic cylinder (shaft) coated with another material as shown in Fig. 3. The model is free to expand or contract under the thermal loading, except that the rigid-body motion is suppressed (the four boundary points on the $x-$ and $y-$ axes are constrained in the tangential directions). The material constants used in this case are:

for the elastic cylinder,

$E = 4.0$ GPa,

$v = 0.34$,

$\alpha = 10.0 \times 10^{-6}/°C$;

for the coating,

$E = 6.0$ GPa,

$v = 0.22$,

$\alpha = 20.0 \times 10^{-6}/°C$.

The temperature change is $\Delta T = 100 °C$.

One BEM mesh and one FEM mesh of the coated cylinder are shown in Fig. 4 (a) and (b), respectively. The density of the FEM mesh is mainly controlled by the thickness of the coating for which two layers of elements are used. Because of the aspect ratio constraints on the FEM mesh, the element size in the circumferential direction cannot be too large for the coating. In addition, elements with comparable size to that of the elements in

Table 1 : BEM results for the thermal stresses in the films of different thickness.

$h(\times L)$	Stress σ_y at node A (MPa)	Stress σ_x at node B (MPa)
1.0	- 12.5000	- 12.5000
10^{-1}	- 12.5000	- 12.5000
10^{-2}	- 12.5000	- 12.5000
10^{-3}	- 12.5000	- 12.5000
10^{-4}	- 12.5000	- 12.5000
10^{-5}	- 12.5000	- 12.5000
10^{-6}	- 12.5000	- 12.5000
10^{-7}	- 12.5000	- 12.5000
10^{-8}	- 12.5000	- 12.5000
10^{-9}	- 12.5000	- 12.5000
10^{-10}	- 12.5000	- 12.5000
10^{-11}	- 12.4932	- 12.5109
10^{-12}	- 12.4992	- 12.5025
10^{-13}	- 12.4997	- 12.4993
10^{-14}	- 12.4996	- 12.5092
10^{-15}	- 12.4994	- 12.3919
10^{-16}	- 12.4996	- 12.6128
Analytical solution	- 12.5	- 12.5

(a)   (b)
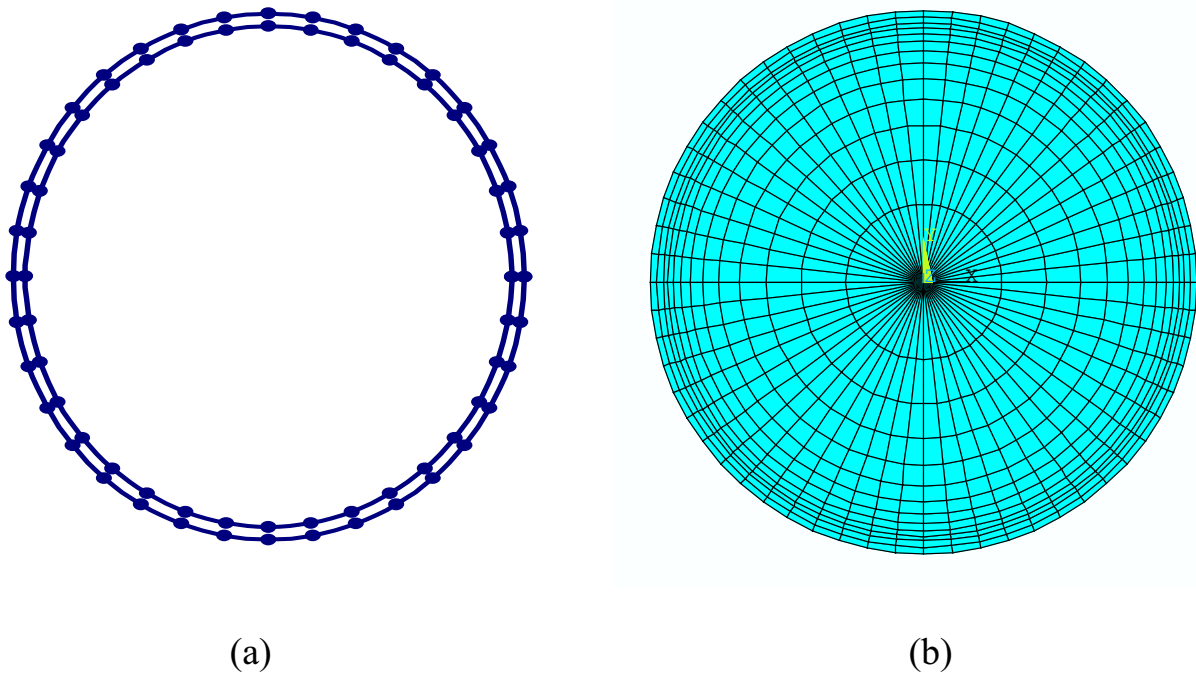
Figure 4 : Discretizations of the elastic cylinder with a thin coating ($h = 0.05a$):
(a) BEM mesh (36 quadratic line elements); (b) FEM mesh (780 quadratic area elements).

```
1                                                          ANSYS 5.6
                                                          NOV  7 2000
                                                          18:17:47
                                                          ELEMENT SOLUTION
                                                          STEP=1
                                                          SUB =1
                                                   MN     TIME=1
                                                          S1        (NOAVG)
                                                          PowerGraphics
                                                          EFACET=1
                                                          DMX =.001512
                                                          SMN =10549
                                                          SMX =334644
                                                              10549
                                                              46560
                                                              82571
                                                              118581
                                                              154592
                                                              190602
                                                              226613
                                                              262623
                                                              298634
                                                              334644
```
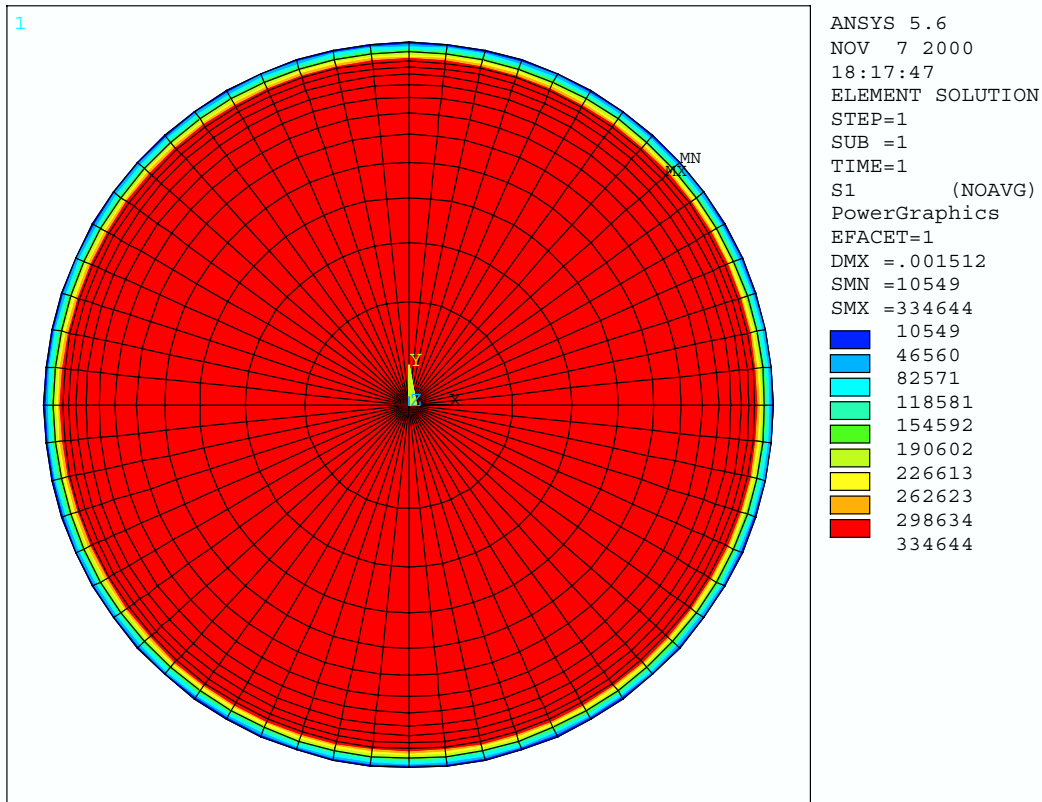
Figure 5 : Contour plot of the radial stress from the FEM solution.

Table 2 : BEM results for the cylinder (a = 1.0 m) with coatings of different thickness.

h(m)	BEM/FEM	No. of elements	u_r at point A (m)	σ_r at point B (Pa)
0.05	BEM	24	0.00151243	325156
		36	0.00151235	323517
		48	0.00151234	323189
	FEM	480	0.00151230	323040
		780	0.00151230	323040
0.03	BEM	24	0.00144405	201602
		36	0.00144397	199916
		48	0.00144396	199515
0.01	BEM	24	0.00137491	70233.0
		36	0.00137486	68977.8
		48	0.00137485	68627.6
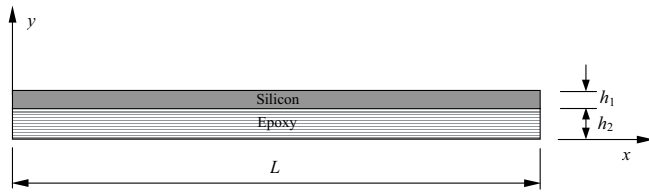
Figure 6 : A two-layer thin film system.

Figure 7 : Results of the normal (peel) stress at the interface using the BEM ($h_1 = 0.66$ mm).

the coating are needed for the cylinder in the region near the interface. Based on these considerations, the FEM mesh generated consists of 780 elements (Fig. 4 (b)) for the case $h = 0.05a$. A FEM mesh (not shown) with a smaller number of elements (480) is achievable by reducing five layers of elements for the cylinder in the radial direction. However, for smaller thickness of the coating, it will be very difficult to generate an FEM mesh with a reasonable number of elements due to the constraints mentioned above. For this reason, the FEM is attempted only for the case of $h = 0.05a$. The commercial software *ANSYS* is used for the FEM analysis.

Table 2 shows the radial displacement of the boundary and the interface normal stress for different thickness of the coating. The BEM results converged quickly with very few elements on the boundary and interface of the two materials for all the three cases studied, while the FEM results converge also for the case $h = 0.05a$, as shown in Table 2. A stress contour plot for the FEM solution (with 780 elements) is shown in Fig. 5. The high accuracy in solution and efficiency in modeling by using the BEM for small thickness of the coating, compared with the FEM, are evident from this example.

3.3 Multi-layer thin films

Finally, we consider a two-layer thin film system, shown in Fig. 6. The two layers are made of silicon (top layer) and epoxy (bottom layer), and the dimensions are $L = 22.0$ mm, $h_2 = 1.0$ mm and h_1 varies from 0.66 mm to 0.1 mm. The bottom edge of the model is fixed and the material constants used are:

for silicon,

$E = 165.0$ GPa,
$\nu = 0.25$,
$\alpha = 3.0 \times 10^{-6}/^{\circ}C$;

for epoxy,

$E = 23.5$ GPa,

$\nu = 0.30$,
$\alpha = 15.0 \times 10^{-6}/^{\circ}C$.

Again, the temperature change is $\Delta T = 100\,^{\circ}C$.

The stress distribution along the interface of the two materials under the thermal loading is investigated first. Fig. 7 shows the normal (peel) stress at the interface from $x = 0$ (left edge) to $x = 11$ mm (center), for $h_1 = 0.66$ mm, using the developed BEM with increasingly larger numbers of boundary elements. The BEM results converge very quickly on the interface away from the edge ($x > 1.0$ mm), with values from about 0.4 MPa in the center to 11 MPa at $x = 1.0$ mm. However, the results converge much slower near the edge ($x = 0$) of the interface due to the singularity of stresses at the edge of a bi-material interface (see, Ref. (Liu, Suo et al. 1999) and the references therein). A BEM mesh with 196 elements, which uses more elements on the interface near the edge by non-uniformly distributing the nodes, is attempted and better results are obtained. Still, the BEM results for $x < 0.5$ mm are deemed unreliable due to the singular nature of the stress fields which oscillate very rapidly near the edge.

The effect of the thickness of the film on the interface stress distributions is studied next. Fig. 8 shows the peel stress for three different thickness of the top film, from 0.66 mm to 0.1 mm. For all the cases, the BEM mesh with 196 elements is used and the nodes on the interface are distributed non-uniformly in order to place more nodes near the two edges. From the results in
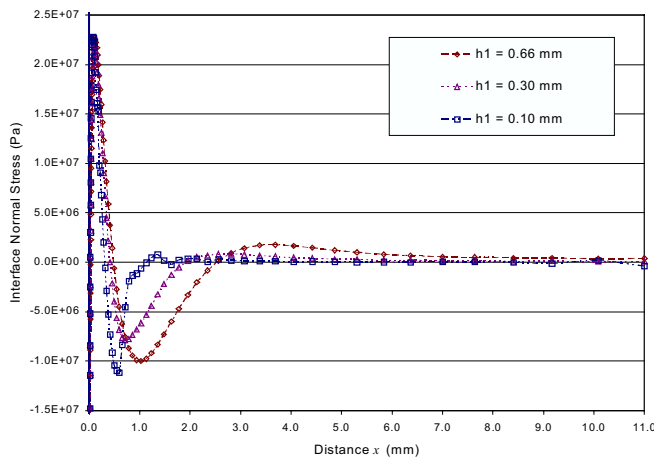
Figure 8 : Peel stress at the interface for different values of h_1 (with 196 elements, non-uniform distribution).
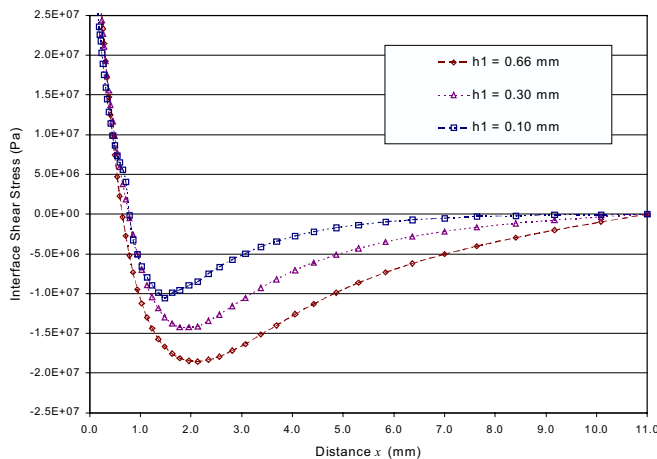
Figure 9 : Shear stress at the interface for different values of h_1 (with 196 elements, non-uniform distribution).

Fig. 8, it seems that there are little changes of the peel stresses in the middle part of the interface as the thickness of the top film decreases. However, the results show that the onset of the oscillation for the peel stresses is pushed toward the edges of the interface as the thickness decreases. Fig. 9 shows the shear stresses at the interface for the three different thicknesses of the top film. Note that the magnitudes of the shear stresses are much larger than those of the peel stresses near the edge ($x = 1.0 \sim 3.0$ mm). The positive sign of the shear stress near the edge ($x = 0$) is reasonable since the top film has a smaller coefficient of thermal expansion. The bottom film expands more compared with the top film, which will cause the top film to "pull back" the edge of the

lower film along the interface direction. Again, the quantitative results for $x < 0.5$ mm are deemed unreliable due to the edge singularity.

4 Discussion

The advanced BEM developed earlier for analyzing thin shell-like and layered structures under mechanical loading is extended in this paper to deal with the thermal loading which has great potentials in applications for thin films or coatings. The developed BEM demonstrates greater accuracy, stability and efficiency in modeling as compared with the FEM in dealing with structures with thin-layers. It is found that when the thickness of a film or coating is changed, the BEM mesh can be updated easily, while for the FEM totally different meshes need to be generated for different material thicknesses. When the thickness is relatively small, an extremely large number of elements need to be used in the FEM model. Hence, using the FEM may not even be feasible to analyze such problems, if the computing resources are limited. With much fewer boundary (line) elements, the BEM can effectively model thin films and coatings with the thickness-to-length ratios down to 10^{-9} (say, in the nano-scale).

However, it should be pointed out that, at present, the developed thermal BEM solver could run several times slower than the commercial FEM for large BEM models, as revealed in Ref. (Chen and Liu 2001). This is due to the fact that a lot of numerical integrations need to be done in the BEM approach in order to form the coefficient matrix and these integrations must be done accurately to ensure the accuracy of the BEM results. Optimization of the integration process and solution methods in the BEM is possible, such as using the new multipole expansion techniques (see, e.g., (Peirce and Napier 1995; Gomez and Power 1997; Fu, Klimkowski et al. 1998; Mammoli and Ingber 1999; Nishimura, Yoshida et al. 1999)) and the iterative solvers (see, e.g., (Freund and Nachtigal 1996; Chen, Liu et al. 2000) and the references therein). These investigations are under way in order to improve the solution efficiency of the developed BEM. On the other hand, the commercial FEM software has been improved significantly over the years, and thus has been very much optimized regarding the solution efficiency. Even if the optimized BEM still runs slower than an FEM software, the efficiency of the BEM in the modeling stage (human time) can well offset the longer time

in the solution process (computer time). The convenience of the BEM in handling the shell-like structures (Krishnasamy, Rizzo et al. 1994; Liu 1998; Luo, Liu et al. 1998; Chen and Liu 1999; Luo, Liu et al. 2000), and the accuracy of the BEM, make the BEM a very attractive, at lest an alternative, numerical tool for the analysis of such materials or structures. With further improvements and the development of an easy-to-use graphical-user interface (GUI) for the developed BEM, it can become an efficient, accurate, and yet robust numerical analysis tool for the materials research and development.

The developed thermal BEM in this paper for analyzing thin layered structures or materials under the thermal loading can also be employed to investigate other more important and realistic problems for thin film, coating and composite materials, such as residual stresses, interfacial crack initiation and propagation (peeling-off), in electronic packaging or other engineering applications. Some of the investigations are already underway.

5   Conclusion

The boundary integral equation formulation for the analysis of thermoelasticity problems is reviewed in this paper. A special form of the BIE is selected for the case of uniform temperature changes, which are adequate for the study of structures or materials with small dimensions, such as thin films or coatings, under the steady-state thermal loading. The techniques developed earlier to handle the nearly-singular integrals existing in the BIE/BEM when applied to thin shell-like structures are extended to deal with the new integrals in thermal loading case. Test problems on thin films and coatings under plane strain conditions are studied and excellent BEM results are obtained. It is demonstrated that the developed thermal BEM can provide accurate and efficient solutions for the analysis of thin films or coatings with the thickness-to-length ratios down to 10^{-9} (the nano-scale), using much fewer boundary elements, as compared with the FEM.

References

Abedian, A., W. Szyszkowski and S. Yannacopoulos (1999). "Effects of surface geometry of composites on thermal stress distribution: a numerical study." *Composites Science and Technology* **59**(1): 41-54.

Banerjee, P. K. (1994). *The Boundary Element Methods in Engineering*. New York, McGraw-Hill.

Brebbia, C. A. and J. Dominguez (1989). *Boundary Elements - An Introductory Course*. New York, McGraw-Hill.

Chen, S. H. and Y. J. Liu (1999). "A unified boundary element method for the analysis of sound and shell-like structure interactions. I. Formulation and verification." *Journal of the Acoustical Society America* **103**(3): 1247-1254.

Chen, S. H., Y. J. Liu and X. Y. Dou (2000). "A unified boundary element method for the analysis of sound and shell-like structure interactions. II. Efficient solution techniques." *Journal of the Acoustical Society America* **108**(6): 2738-2745.

Chen, X. L. and Y. J. Liu (2001). "Multiple-cell modeling of fiber-reinforced composites with the presence of interphases using the boundary element method." *Computational Materials Science* **21**(1): 86-94.

Cheng, W. H., Y. D. Yang, T. C. Liang, G. L. Wang, et al. (1999). "Thermal stresses in box-type laser packages." *Optical and Quantum Electronics* **31**(4): 293-302.

Cruse, T. A. (1974). "An improved boundary-integral equation method for three dimensional elastic stress analysis." *Computers & Structures* **4**: 741-754.

Cruse, T. A. (1988). *Boundary Element Analysis in Computational Fracture Mechanics*. Dordrecht, The Netherlands, Kluwer Academic Publishers.

Cruse, T. A. and R. Aithal (1993). "Non-singular boundary integral equation implementation." *International Journal for Numerical Methods in Engineering* **36**: 237-254.

Freund, R. W. and N. M. Nachtigal (1996). "QMRPACK: a package of QMR algorithms." *ACM Transactions on Mathematical Software* **22**(March): 46-77.

Fu, Y., K. J. Klimkowski, G. J. Rodin, E. Berger, et al. (1998). "A fast solution method for three-dimensional many-particle problems of linear elasticity." *International Journal for Numerical Methods in Engineering* **42**: 1215-1229.

Gomez, J. E. and H. Power (1997). "A multipole direct and indirect BEM for 2D cavity flow at low Reynolds number." *Engineering Analysis with Boundary Elements* **19**: 17-31.

Gray, L. J., D. Maroudas and M. N. Enmark (1998). "Galerkin boundary integral method for evaluating surface derivatives." *Computational Mechanics* **22**(2): 187-193.

Gray, L. J., D. Maroudas, M. N. Enmark and E. F. D'Azevedo (1999). "Approximate Green's functions in boundary integral analysis." *Engineering Analysis with Boundary Elements* **23**(3): 267-274.

Hu, S. Y., Y. L. Li, D. Munz and Y. Y. Yang (1998). "Thermal stresses in coated structures." *Surface & Coatings Technology* **99**(1-2): 125-131.

Huang, Q. and T. A. Cruse (1993). "Some notes on singular integral techniques in boundary element analysis." *International Journal for Numerical Methods in Engineering* **36**: 2643-2659.

Igic, P. M. and P. A. Mawby (1998). "Finite element modelling of the thermal stress field during processing of VLSI multilevel structures." *Electronics Letters* **34**(5): 471-472.

Igic, P. M. and P. A. Mawby (1999). "An advanced finite element strategy for thermal stress field investigation in aluminum interconnections during processing of very large scale integration multilevel structures." *Microelectronics Journal* **30**(12): 1207-1212.

Kane, J. H. (1994). *Boundary Element Analysis in Engineering Continuum Mechanics*. Englewood Cliffs, NJ, Prentice Hall.

Katsikadelis, J.T. and M.S. Nerantzaki (2000). "A boundary-only solution to dynamic analysis of non-homogeneous elastic membranes" *CMES: Computer Modeling in Engineering & Sciences*, **1**(3): 1-10.

Krishnasamy, G., F. J. Rizzo and Y. J. Liu (1994). "Boundary integral equations for thin bodies." *International Journal for Numerical Methods in Engineering* **37**: 107-121.

Liu, X. H., Z. G. Suo and Q. Ma (1999). "Split singularities: Stress field near the edge of a silicon die on a polymer substrate." *Acta Materialia* **47**(1): 67-76.

Liu, Y. J. (1998). "Analysis of shell-like structures by the boundary element method based on 3-D elasticity: formulation and verification." *International Journal for Numerical Methods in Engineering* **41**: 541-558.

Liu, Y. J. (2000). "On the simple-solution method and non-singular nature of the BIE/BEM - A review and some new results." *Engineering Analysis with Boundary Elements* **24**(10): 787-793.

Liu, Y. J. and T. J. Rudolphi (1991). "Some identities for fundamental solutions and their applications to weakly-singular boundary element formulations." *Engineering Analysis with Boundary Elements* **8**(6): 301-311.

Liu, Y. J. and N. Xu (2000). "Modeling of interface cracks in fiber-reinforced composites with the presence of interphases using the boundary element method." *Mechanics of Materials* **32**(12): 769-783.

Liu, Y. J., N. Xu and J. F. Luo (2000). "Modeling of interphases in fiber-reinforced composites under transverse loading using the boundary element method." *Journal of Applied Mechanics* **67**(1 (March)): 41-49.

Liu, Y. J., D. M. Zhang and F. J. Rizzo (1993). "Nearly singular and hypersingular integrals in the boundary element method." *Boundary Elements XV*, C. A. Brebbia and J. J. Rencis, Eds., Worcester, MA, Computational Mechanics Publications.

Luo, J. F., Y. J. Liu and E. J. Berger (1998). "Analysis of two-dimensional thin structures (from micro- to nano-scales) using the boundary element method." *Computational Mechanics* **22**: 404-412.

Luo, J. F., Y. J. Liu and E. J. Berger (2000). "Interfacial stress analysis for multi-coating systems using an advanced boundary element method." *Computational Mechanics* **24**(6): 448-455.

Mammoli, A. A. and M. S. Ingber (1999). "Stokes flow around cylinders in a bounded two-dimensional domain using multipole-accelerated boundary element methods." *International Journal for Numerical Methods in Engineering* **44**: 897-917.

Mukherjee, S. (1982). *Boundary Element Methods in Creep and Fracture*. New York, Applied Science Publishers.

Mukherjee, S., M. K. Chati and X. L. Shi (2000). "Evaluation of nearly singular integrals in boundary element contour and node methods for three-dimensional linear elasticity." *International Journal of Solids and Structures* **37**(51): 7633-7654.

Nikiskov, G.P., J.H. Park, and S.N. Atluri (2001). "SGBEM-FEM alternating method for analyzing 3D

non-planar cracks and their growth in structural components" *CMES: Computer Modeling in Engineering & Sciences*, **2**(3): In Print.

Nishimura, N., K.-i. Yoshida and S. Kobayashi (1999). "A fast multipole boundary integral equation method for crack problems in 3D." *Engineering Analysis with Boundary Elements* **23**: 97-105.

Peirce, A. P. and J. A. L. Napier (1995). "A spectral multipole method for efficient solution of large-scale boundary element models in elastostatics." *International Journal for Numerical Methods in Engineering* **38**: 4009-4034.

Rizzo, F. J. (1967). "An integral equation approach to boundary value problems of classical elastostatics." *Quart. Appl. Math.* **25**: 83-95.

Rizzo, F. J. and D. J. Shippy (1977). "An advanced boundary integral equation method for three-dimensional thermoelasticity." *International Journal for Numerical Methods in Engineering* **11**: 1753-1768.